ORIGINAL PAPER

DEVELOPMENT OF THE RAMBERG-OSGOOD MECHANICAL STRESS-STRAIN CURVE USING THE ARTIFICIAL NEURAL NETWORK METHOD TO EVALUATE MECHANICAL BEHAVIOUR OF 316L STAINLESS STEEL IN THE LIQUID LEAD

LIVIA STOICA[1], VASILE RADU[1], ALEXANDRU NITU[1]

Manuscript received: 12.01.2023; Accepted paper: 22.04.2023;
Published online: 30.06.2023.

Abstract. *Romania, through RATEN ICN, is involved in the construction of the ALFRED demonstrator (Advanced Lead Fast Reactor European Demonstrator), in which the core of the reactor uses cooling in the liquid lead environment. This constitutes one of the arguments for the development of studies on innovative materials of generation IV, having the stated objective of the problem of the contact between the liquid lead and the structural materials specific to this type of reactor. The purpose of this paper is to highlight the changes in the thermomechanical behaviour induced by the contact between the 316L austenitic steel and the liquid lead, as well as its modelling through the equation of the Ramberg-Osgood-type mechanical stress-strain curve. The tensile tests in air and liquid lead were carried out at strain rates of the specimens in the range 10^{-3} s^{-1} ~ 10^{-5} s^{-1} and in a range of temperatures 350^{o}C - 400 ^{o}C. To highlight the changes induced by the contact with the liquid lead on the thermomechanical behaviour of the 316L steel, the artificial neural network method, called the "Multilayer Feedforward Neural Network", was used in the processing of the experimental database. The obtained Ramberg-Osgood-type mechanical stress-strain curve is applied for both the air and the liquid lead environment at a temperature of 375^{o}C and includes the following parameters as input: temperature, strain rate, yield stress, and maximum stress at necking. The two equations obtained for the air environment and the liquid lead environment at a temperature of 375^{o}C were verified to the experimental data and a very good prediction agreement was obtained.*

Keywords: *stress-strain Ramberg-Osgood curve; artificial neural network; liquid lead environment; generation IV reactor.*

1. INTRODUCTION

Romania, through RATEN ICN, is involved in the construction of the ALFRED demonstrator (Advanced Lead Fast Reactor European Demonstrator), in which the core of the reactor uses cooling in the liquid lead environment. This constitutes one of the arguments for the development of studies on innovative materials of generation IV, having the stated objective of the problem of the contact between the liquid lead and the structural materials specific to this type of reactor. Thus, the purpose of this work is to highlight the changes in the thermomechanical behaviour induced by the contact between the 316L austenitic steel with liquid lead, as well as its modelling through the equation of the Ramberg-Osgood-type mechanical stress-strain curve. It should be noted that there are still no systematic studies in

[1] RATEN Institute for Nuclear Research, Department of Nuclear Material and Corrosion, Pitesti, Romania.
E-mail: livia.stoica@nuclear.ro.

the specialized literature carried out for the evaluation of the thermomechanical behaviour of 316L steel under tensile mechanical stress in the liquid lead environment, in the range of temperatures 350°C – 400°C. Therefore, the present study's scientific approach focuses on obtaining the mentioned material constitutive equations. However, few liquid metal embrittlement (LME) models, according to the main features, support, gaps from reference [1] are displayed in Table 1.

Table 1. Models for liquid metal embrittlement

Model	The main features	Model support	Limitations	Constitutive equation $\sigma \sim \varepsilon$
Reduction in Surface Energy	Thermodynamic approach, the defect is usually intergranular	Experimental support, consider the effects of experimental observations	Does not take into account the mechanisms of atomic degradation	No
Adsorption Induced Reduction in Cohesion	Adsorption of liquid metal reduces the strength of cohesion on the atomic planes	Qualitatively consider the effects of many experimental observations Fractographic support	No more experimental observations can be explained	No
Enhanced Dislocation Emission	Defect occurs by localized micro- ductile coalescence	Experimental support, strong fractographic support	No math analysis, based on complicated fractographic analyzes	No
Enhanced Work Hardening	Adsorption of liquid metal atoms facilitates dislocation motion	Experimental support for discontinuous crack growth	No math analysis, Lack of experimental support for improved hardening	No
Localized plasticity that favors LME	Liquid metal diffuses along the grain boundary before the crack tip	Correctly predicts that LME rupture is accompanied by extensive plasticity	Lack of experimental support	No
Dissolution-Condensation	Crack growth by the stress-assisted dissolution of solid metal into liquid metal at the tip of the crack	Limited experimental support	Predicts the wrong dependence of LME on the composition of liquid metals	No
Grain Boundary Penetration	Promoted stress diffusion of the liquid metal along the grain boundaries before the crack tip	Can qualitatively consider the effects of many experimental observations,	No math analysis, lack of experimental support	No
Present study	**Adsorption of liquid metal reduces the strength of cohesion in front of microcracks**	**Experimental support, strong fractographic support**	**Does not take into account the oxygen effect in the liquid lead on LME**	**Yes Ramberg-Osgood**

From the Table 1, one may see that present paper fills the main gap concerning of constitutive equation, by Ramberg-Osgood type mechanical stress-strain curve model, that is developed based on the experimental results carried out in the liquid lead environment, and in the air environment as well.

In the structural integrity analyses performed using programs based on the finite element method, it is necessary to specify the material constitutive equations as a mandatory input requirement. Although the mechanical demands in the design for a structural component are in the elastic domain, there are situations when material discontinuities, initial defects or developed during operation may appear, which constitute high mechanical stress spots. In

other words, although in the volume of the material the mechanical stresses can be in the elastic domain, locally they are in the elastoplastic domain, and the analysis of the field of mechanical stresses and strains must be performed properly with the finite element method or with analytical or engineering methods. For the analysis of the field of mechanical stresses, which is located in the elastoplastic field, the constitutive equation of mechanical stress-deformation must be specified over a wide range of deformations, and this can be chosen in several ways, one of them being the Ramberg-Osgood representation of mechanical tension - deformation curves. To describe the behaviour of the coefficient of hardening of material deformation, using experimental curves of mechanical tension versus material deformation, different methods are reported in the scientific literature.

In the reference [2] a program that fits the analytical expressions with the experimental mechanical stress-strain data to describe the Ramberg-Osgood equation is described. Quantities resulting from data processing are based on yield stress, plastic strain component, tangent modulus of plastic strain, and Poisson's ratio value. The reverse engineering methodology described in reference [3] proposed obtaining the strain hardening and strength coefficients for the tensile test. A generalized approach [4] uses plastic strain value corresponding to Luder's strain along with engineering yield stress and ultimate tensile strength to estimate the strain hardening exponent in the Ramberg-Osgood type of true stress-true strain relationship.

In the paper, a Ramberg-Osgood type mechanical stress-strain curve model is developed based on the experimental results carried out in the liquid lead environment, and in the air environment as well. This allows obtaining some analytical equations for the coefficients of the equation of the Ramberg-Osgood type mechanical stress-strain curve. Chapter 2 presents the installation and methodology for performing mechanical tensile tests in air and in liquid lead, using specific 316L stainless steel specimens. Chapter 3 describes obtaining the parameters of the Ramberg-Osgood-type mechanical stress-strain curve equation and analyzes the obtained experimental database. To highlight the changes induced by the contact with the liquid lead on the thermomechanical behaviour of the 316L steel, the artificial neural network method of the "Multilayer Feedforward Neural Network" type, was used in the processing of the experimental database, this being the subject of chapter 4. In chapter 5, the equations obtained for the Ramberg-Osgood type mechanical stress-strain curve, are applied for the air environment and the liquid lead environment at a temperature of 375°C and include as input the following parameters: temperature, deformation rate, yield stress, maximum stress at necking. It was verified against the experimental data and a good prediction agreement was obtained. The elaborated model has practical utility in the structural integrity analysis of the various components made of 316L steel in the ALFRED reactor.

2. SLOW STRAIN RATE TESTING OF 316L STAINLESS STEEL IN THE AIR AND IN THE LIQUID LEAD ENVIRONMENT

The experimental tests were carried out on an INSTRON-type testing machine on which the experimental facilities for testing in the liquid lead environment were developed. Thus, the uniaxial tensile tests on specific specimens made of 316L austenitic steel were carried out in the air and in the liquid lead. Testing in the liquid lead environment is based on a crucible containing, under static conditions, liquid lead, with temperatures up to 450°C. A system for monitoring dissolved oxygen in the liquid lead had not yet been implemented at the time of the tensile tests for this study. The entire experimental setup developed for the liquid lead testing, together with the INSTRON traction machine, is shown in Fig. 1a.

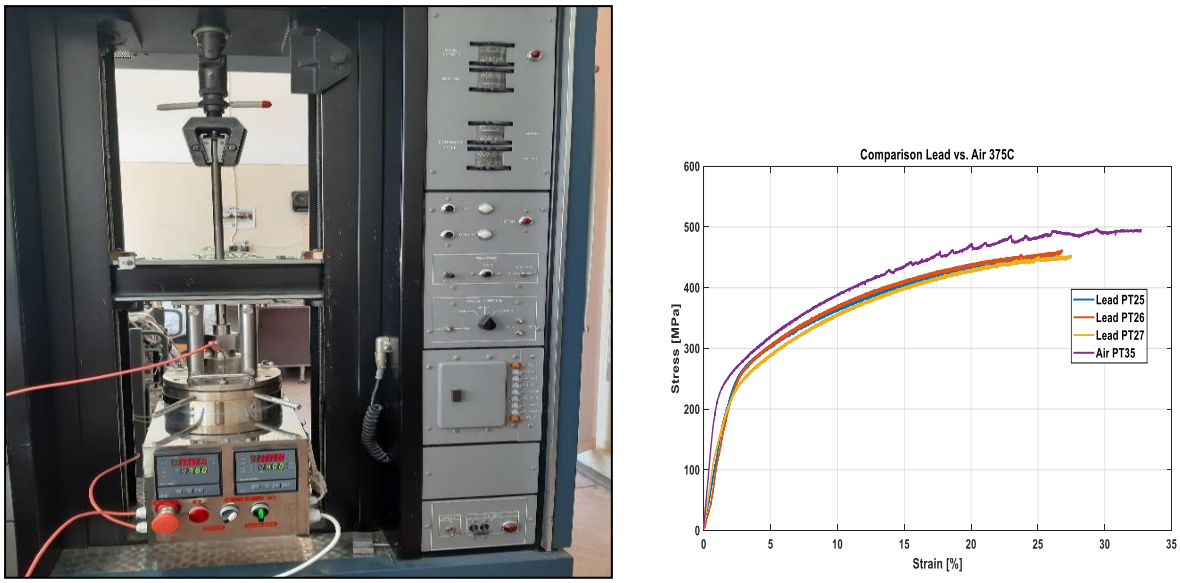

(a) (b)

Figure 1. Experimental test setup in the liquid lead environment (a) and tensile stress-strain curves in air and lead 375ºC, and strain rate of $5 \times 10^{-5} s^{-1}$ (b).

The tensile tests in air and liquid lead were carried out at deformation rates of the sample in the range 10^{-3} s^{-1} ~ 10^{-5} s^{-1}, following ASTM G129 [5] and ASTM E8 [6], in a temperature range of 350°C - 400°C. The diagrams obtained during the "Slow Strain Rate Testing" (SSRT) tests were converted into real mechanical stress-strain curves. Figure 1(b) shows a set of curves $\sigma = f(\varepsilon)$, which were represented up to the necking points of interest, points where the tangents to these curves take zero value. At a first comparative analysis of these results, several elements related to the effect on the thermomechanical behaviour of steel in the liquid lead environment can be found. For the tests performed in the liquid lead environment, a systematic decrease in ductility was observed, by reducing the total deformation compared to the tests performed in the air environment. At the same time, there is also a decrease in the fracture strength as well as in the yield stress for the test in liquid lead, which can also be attributed to the effect of liquid lead on the 316L specimens, the tensile test being of the SSRT type. This means that the effect of the liquid lead environment on the thermomechanical behaviour of the 316L austenitic steel specimens cannot be neglected at these tensile strain rates and temperatures range.

3. THE EXPERIMENTAL RESULTS DATABASE USED FOR THE RAMBERG – OSGOOD STRESS-STRAIN CURVE EQUATION MODELLING

The Ramberg–Osgood plastic yield rule [7] states that, for quasi-static loading at a given temperature and strain rate, the actual mechanical stress is given by the strength coefficient *K*, the strain-hardening exponent *n*, and the actual plastic strain:

$$\sigma = K\varepsilon_p^n \tag{1}$$

here: *n* - strain hardening exponent and *K* - strength coefficient.

The instability that occurs in a specimen under increase of the mechanical loading is known as the phenomenon of "localized deformation". Localized deformation is generally initiated at maximum load during tensile deformation of a ductile metal [7].

The strain at which localized strain occurs is numerically equal to the strain hardening coefficient [7]:

$$\varepsilon_u = n \tag{2}$$

Based on this statement, in previous our work [8] a new method has been proposed for obtaining the deformation hardening coefficient, from the mechanical stress-strain curve. The relation (1), which describes the flow curve, can be written for the pair of values at the yield limit ($\sigma_{0.2}, \varepsilon_{0.2}$) and the pair of values at the localized strain (σ_u, ε_u):

$$\sigma_{0.2} = K \cdot \varepsilon_{0.2}^{n}. \tag{3}$$

Respectively,

$$\sigma_u = K \cdot \varepsilon_u^{n} \tag{4}$$

From the relation (3) and (4) it is obtained:

$$\frac{\sigma_u}{\sigma_{0.2}} = \left(\frac{\varepsilon_u}{\varepsilon_{0.2}}\right)^{n} \tag{5}$$

and by logarithm:

$$ln\left(\frac{\sigma_u}{\sigma_{0.2}}\right) = n[ln(\varepsilon_u) - ln(\varepsilon_{0.2})] \tag{6}$$

Taking into account relation (2) results in a transcendental equation for the hardening exponent:

$$ln\left(\frac{\sigma_u}{\sigma_{0.2}}\right) = n[ln(n) - ln(\varepsilon_{0.2})] \tag{7}$$

Equation (7) is solved numerically in the MATLAB programming environment [9]. Since $\sigma_{0.2}$ it represents the mechanical stress with a plastic deformation of 0.2%, it follows:

$$\alpha = \frac{0.002 \cdot E}{\sigma_{0.2}} \tag{8}$$

In the present paper, the experimental tensile mechanical tension-deformation curves will be processed according to the Ramberg - Osgood model. From practical considerations, related to the use of the constitutive equation in the analysis with the finite element method, the equation of the stress-strain curve in the Ramberg – Osgood format has the form:

$$\frac{\varepsilon}{\varepsilon_0} = \frac{\sigma}{\sigma_0} + \alpha \cdot \left(\frac{\sigma}{\sigma_0}\right)^{m} \tag{9}$$

characterized by parameters α , respectively $m = 1/n$, which is the inverse of the hardening exponent.

As it was already mentioned previously, the experimental tests were performed on 316L stainless steel samples at sample strain rates in the range $\dot{\varepsilon} = (10^{-3}, 10^{-5})s^{-1}$, following ASTM G129 [5] and ASTM E8 [6], in a temperature range between 350°C and 400°C. Using the methodology described above, from the curves $\sigma = f(\varepsilon)$ the following quantities were extracted: the coefficient α of the Ramberg-Osgood relation, the parameter m, which is the inverse of the hardening exponent, n. At the same time, the database also contains the yield stress values, $\sigma_{0.2}$, respectively of the maximum stress corresponding to the localized deformation, σ_u , which were determined for all tested specimens.

Fig. 2 shows the values obtained for the coefficient α of the Ramberg-Osgood relationship following tests performed in the air on 316L stainless steel samples, as well as the parameter m, which is the inverse of the hardening exponent, n.

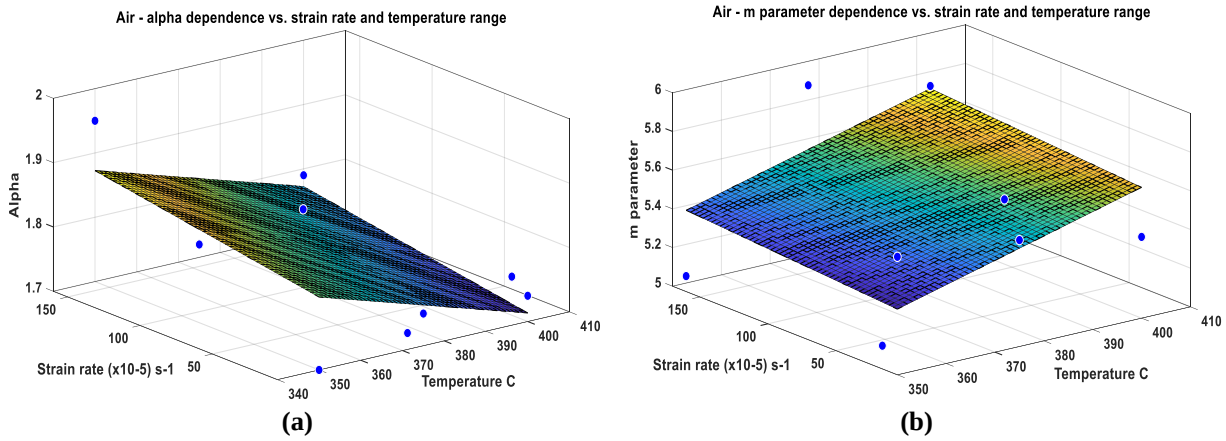

(a) **(b)**

Figure 2. Dependence of the coefficient α of the Ramberg-Osgood relationship (a) and of the parameter m, - which is the inverse of the roughening exponent, n (b), depending on the strain rate in the temperature range 350°C -400°C in air.

From the above analysis of the dependencies suggested by the interpolation surfaces represented in Fig. 2, the following can be found:

- for the coefficient α of the Ramberg - Osgood equation, for the entire temperature range (350°C – 400°C), the value of the parameter α decreases slightly with the increase of the strain rate; with the increase in temperature, regardless of the strain rate, the value of the parameter decreases;
- for the parameter m of the Ramberg – Osgood equation, for the entire temperature range (350°C – 400°C), the value of the parameter m decreases slightly with the increase of the strain rate; with increasing temperature, regardless of the deformation rate, the value of the parameter increases.

Fig. 3 shows the values obtained from the tests performed in the liquid lead environment on 316L stainless steel samples for the coefficient α of the Ramberg-Osgood relationship, and the parameter m, which is the inverse of the hardening exponent, n.

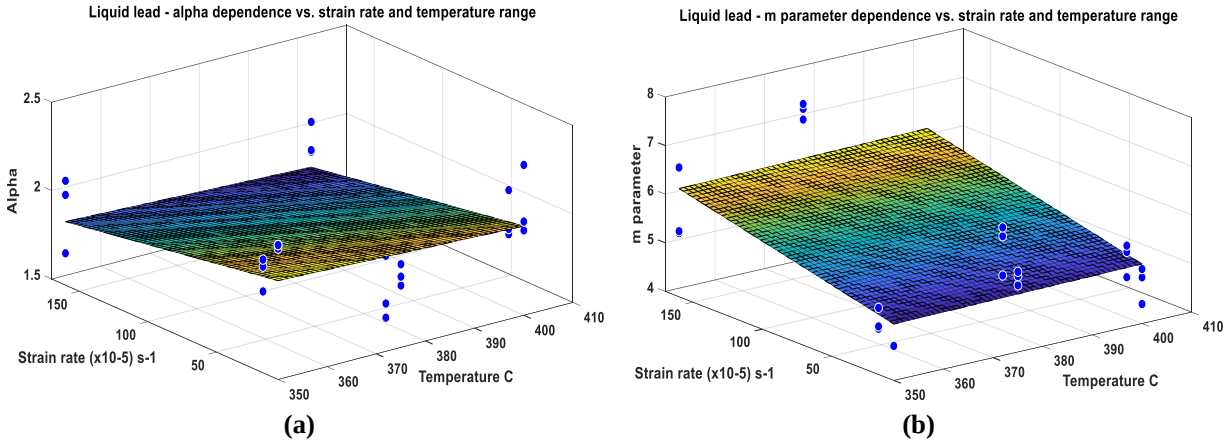

(a) **(b)**

Figure 3. Dependence of the coefficient α of the Ramberg-Osgood relationship (a) and of the parameter m, which is the inverse of the hardening exponent, n (b), depending on the strain rate in the temperature range 350°C - 400°C in the liquid lead.

From the analysis of the dependencies suggested by the interpolation surfaces represented in Fig.3, the following can be found:

- for the parameter α of the Ramberg-Osgood equation, in the tests performed in liquid lead, for the entire temperature range (350°C - 400°C), the value of the parameter α remains almost constant at each value of the strain rate; the same can be said for the dependence of the strain rate at a given temperature value;

- for the parameter m of the Ramberg - Osgood equation, in the tests performed in the liquid lead for the entire temperature range (350°C – 400°C), the value of the parameter m decreases significantly with the increase of the deformation speed; with increasing temperature, the value of the parameter m remains almost constant for a given value of the strain rate.

The experimental database also contains the yield limit values, $\sigma_{0.2}$, respectively of the maximum load corresponding to the localized deformation, σ_u, determined for all tested samples, shown in Figs. 4 and 5, respectively.

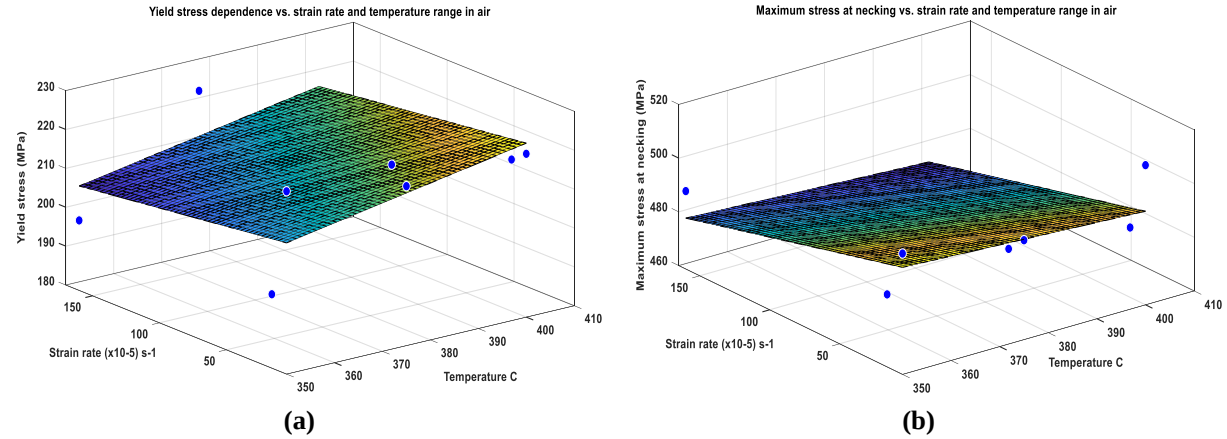

(a) **(b)**

Figure 4. Yield stress (a) and maximum stress corresponding to localized deformation (b), for 316L steel depending on the strain rate in the temperature range 350°C - 400°C in air.

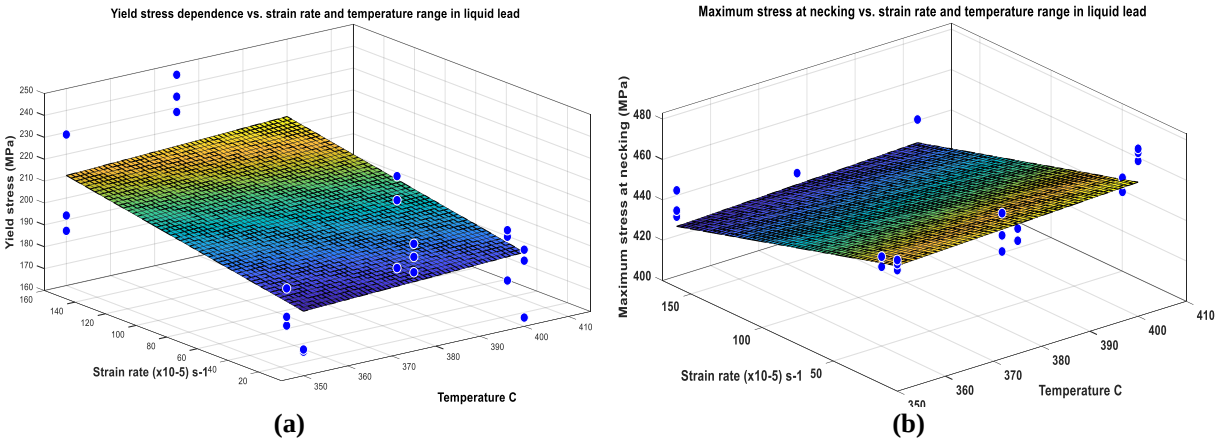

Figure 5. Yield stress (a) and maximum stress corresponding to localized deformation (b), for 316L steel depending on the strain rate in the temperature range 350°C - 400°C in the liquid lead.

It can be seen from the above analysis of Figs. 2-5, a considerable scattering both for the calculated values of the parameters α and m as well as for the yield limit values, respectively the maximum stress at necking obtained in the tests performed in liquid lead. This constitutes an additional reason for the option of modelling by the method of artificial neural networks, which will be presented in the next chapter.

4. MULTILAYER FEEDFORWARD NEURAL NETWORK USED TO MODEL THE PARAMETERS FOR RAMBERG-OSGOOD STRESS-STRAIN CURVE EQUATION

The methodology of artificial neural networks has been used since the 1990s in material modelling [10-12]. Modelling through artificial neural networks is radically different from that based on mathematical modelling. The information on the behaviour of the materials contained in the experimental databases is used directly by the artificial neural network models. For these models in the methodology of artificial neural networks, there is no need for idealizations, as is normally done in mathematical modelling. Therefore, the methodology of artificial neural networks allows the description of quite complex relationships between the input parameters and the target parameters [13].

In function approximation, the Multilayer Feedforward Neural Network (MFNN) is probably the most popular network architecture used in nonlinear neural modelling today. In this type of network, each unit takes a weighted sum of the *input* data and passes this activation level through a transfer function. Input data is processed through a one-way network, "forward", passing through successive layers. Fig. 6 shows a simplified flaw chart used for a two-layer *tansig/purelin* MFNN network.

The mathematics behind the artificial neural network fitting tool is quite complex and it is not the subject of present study. For data processing, the Neural Network Toolbox from MATLAB program [9] was used in the present paper . This type of MFNN network will be used for parameter evaluation α and $m = 1/n$ which characterizes the equation of the Ramberg-Osgood type mechanical stress-strain curve. The MFNN neural network model will contain two layers of neurons. We will work with 5 neurons for the hidden layer, and only one neuron will be used for the output layer. For the hidden layer we used the *tansig* transfer function and for the output layer the *purelin* transfer function. After the first initialization and running of the network, the characteristics of the MFNN realization process were analyzed, as follows: data splitting (randomly), training type (*Levenberg-Marquardt*), learning

performance, number of trials (*epochs*) for to reach the best performance, and the number of validation checks.

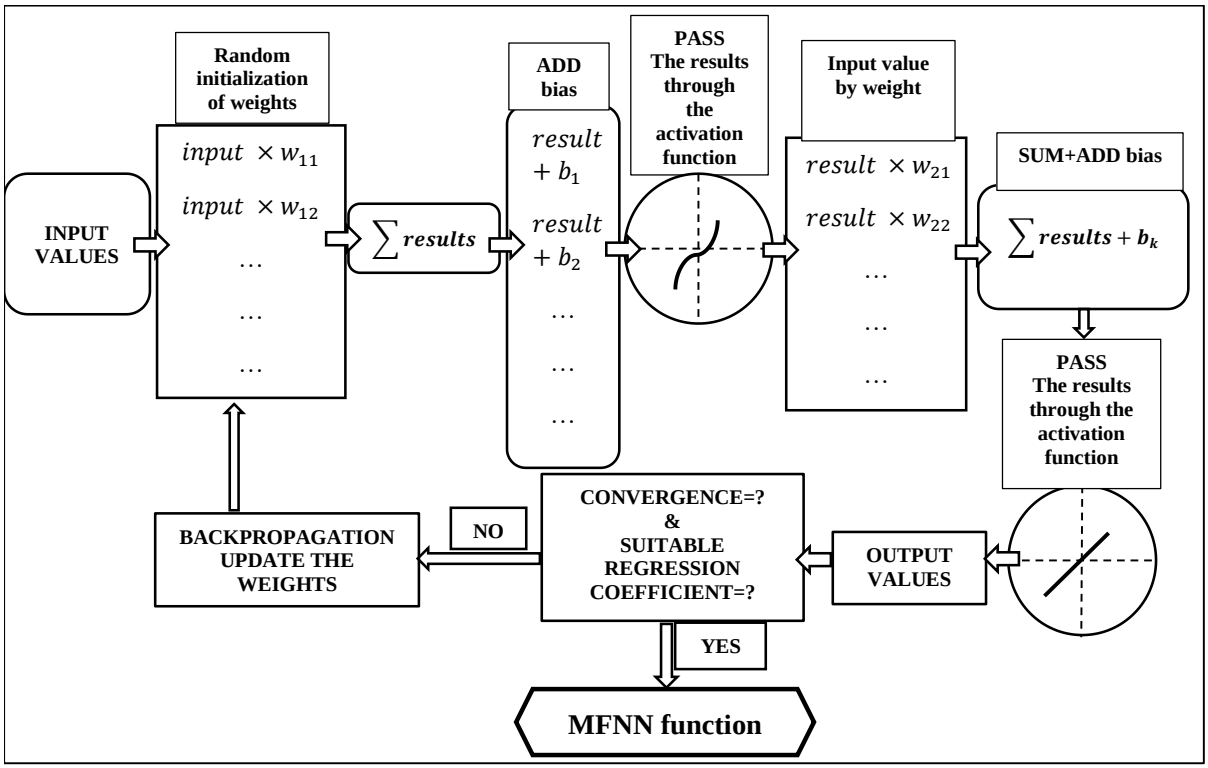

Figure 6. Flaw chart of two-layer tansig/purelin MFNN network

The MFNN model built in the paper for the parameters α and $m = 1/n$, which characterizes the Ramberg – Osgood constitutive equation, accepts as input the following variables: temperature (T), tensile strain rate ($\dot{\varepsilon}$), yield stress ($\sigma_{0.2}$), the maximum stress that determines the localized deformation (σ_u). For this model, the output values are the estimated values of the parameters α and $m = 1/n$ that characterize the equation of the Ramberg-Osgood-type mechanical stress-strain curve. These values were obtained from processing the experimental database and the method presented in chapter 3.

Using the methodology of the artificial neural method of the MFNN type, the explicit functions for the parameters α and m are obtained based on the data contained in the matrices of the test results carried out in the air and liquid lead environments.

Processing of experimental data obtained for 316L steel in the air environment. After processing the data through the MFNN network methodology, the function obtained for the coefficient $\alpha_{air}\ (T, \dot{\varepsilon}, \sigma_{0.2}, \sigma_u)$ has the following form:

$$\alpha_{air}\ (T, \dot{\varepsilon}, \sigma_{0.2}, \sigma_u) =$$
$$= \frac{0.1535199832}{\exp(0.0157169072 \cdot \sigma_{0.2} - 0.06676656384 \cdot \sigma_u - 0.07362022963 \cdot T - 0.1083065326 \cdot \dot{\varepsilon} + 75.29003156) + 1.0}$$
$$- \frac{0.2365077134}{\exp(0.04264235719 \cdot \sigma_u - 0.4544772243 \cdot \sigma_{0.2} - 0.00392211372 \cdot T - 0.008434048107 \cdot \dot{\varepsilon} + 79.34997665) + 1.0}$$
$$+ \frac{0.6325132439}{\exp(50.14925053 - 0.07986180668 \cdot \sigma_u - 0.234652205 \cdot T - 0.05375160671 \cdot \dot{\varepsilon} - 0.03426597872 \cdot \sigma_{0.2}) + 1.0}$$
$$- \frac{2.076965747}{\exp(0.5050429755 \cdot \sigma_{0.2} + 0.2481844408 \cdot \sigma_u - 0.3889452763 \cdot T + 0.2070418955 \cdot \dot{\varepsilon} - 49.10719742) + 1.0}$$
$$- \frac{2.153155082}{\exp(0.2180445427 \cdot \sigma_{0.2} + 0.1479708912 \cdot \sigma_u + 0.1207130135 \cdot T + 0.07089952978 \cdot \dot{\varepsilon} - 123.4715136) + 1.0}$$
$$+ 1.307553795$$

For the parameter $m_{aer}(T, \dot{\varepsilon}, \sigma_{0.2}, \sigma_u)$ the MFNN function is:

$$m_{air}(T, \dot{\varepsilon}, \sigma_{0.2}, \sigma_u) =$$
$$= \frac{1.376823648}{\exp(0.1010589155 \cdot \sigma_u - 0.00903922038 \cdot \sigma_{0.2} - 0.1437156176 \cdot T + 0.01072826591 \cdot \dot{\varepsilon} - 23.45732203) + 1.0}$$
$$- \frac{2.290502637}{\exp(0.1350483712 \cdot T - 0.03574108429 \cdot \sigma_u - 0.1594679465 \cdot \sigma_{0.2} - 0.02427346108 \cdot \dot{\varepsilon} + 32.53306723) + 1.0}$$
$$- \frac{3.027996311}{\exp(0.09500214958 \cdot T - 0.05144939472 \cdot \sigma_u - 0.265195393 \cdot \sigma_{0.2} + 0.05112680995 \cdot \dot{\varepsilon} + 78.1810692) + 1.0}$$
$$- \frac{2.71534429}{\exp(0.1816733758 \cdot T - 0.1041205667 \cdot \sigma_u - 0.09708069808 \cdot \sigma_{0.2} - 0.1315849855 \cdot \dot{\varepsilon} + 48.45071035) + 1.0}$$
$$+ \frac{2.041644833}{\exp(0.02508797134 \cdot \sigma_u - 0.05717042737 \cdot \sigma_{0.2} - 0.0004544975416 \cdot T - 0.00004444304224 \cdot \dot{\varepsilon} + 1.064443306) + 1.0}$$
$$+ 3.508276934$$

The predictions of functions (10) and (11) are represented in Fig. 7, where a good agreement with the corresponding values from the test matrix can be found.

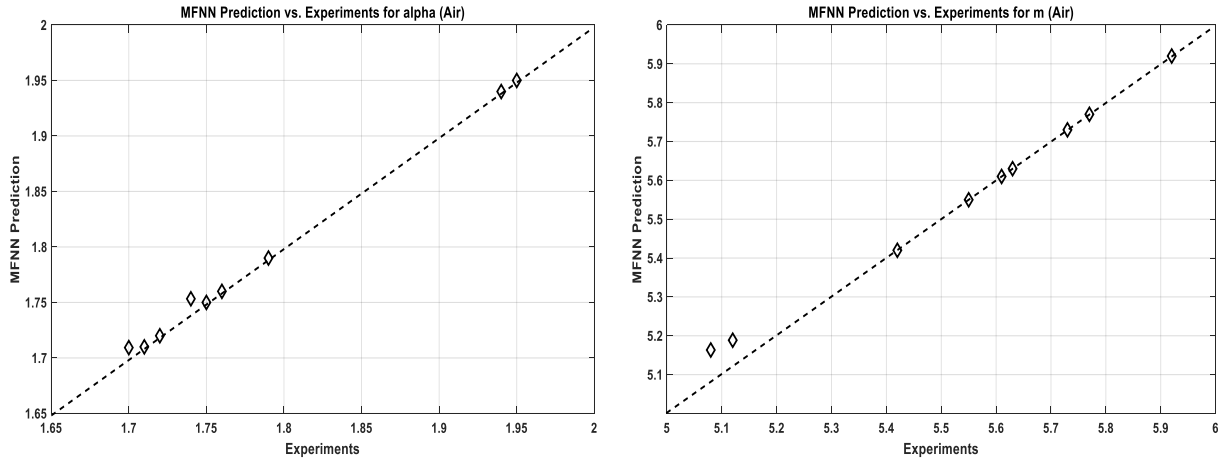

(a) (b)

Figure 7. Predictions of the function $\alpha_{air}(T, \dot{\varepsilon}, \sigma_{0.2}, \sigma_u)$ (a) and of the function $m_{air}(T, \dot{\varepsilon}, \sigma_{0.2}, \sigma_u)$ (b) versus experimental values.

Processing of the experimental data obtained for the 316L steel in the liquid lead environment. For the analysis of the results of the tests performed in the liquid lead environment, the same methodology of artificial neural networks of the MFNN type, implemented in the MATLAB environment, was used.

Thus, for the parameter $\alpha_{lead}(T, \dot{\varepsilon}, \sigma_{0.2}, \sigma_u)$ the corresponding MFNN function is:

$$\alpha_{lead}(T, \dot{\varepsilon}, \sigma_{0.2}, \sigma_u) =$$
$$= \frac{0.01111703549}{\exp(0.1758779686 \cdot \sigma_{0.2} - 0.6841160186 \cdot \sigma_u + 0.4240382537 \cdot T + 0.4211538564 \cdot \dot{\varepsilon} + 73.75522087) + 1.0}$$
$$- \frac{0.4168912674}{\exp(0.4670985643 \cdot \sigma_{0.2} - 0.0421241148 \cdot \sigma_u + 0.3415910184 \cdot T - 0.3131816471 \cdot \dot{\varepsilon} + 19.93870722) + 1.0}$$
$$+ \frac{0.9591262485}{\exp(0.04809159409 \cdot \sigma_{0.2} + 0.003358524713 \cdot \sigma_u - 0.0005350602848 \cdot T + 0.0004271396583 \cdot \dot{\varepsilon} - 10.41126806) + 1.0}$$
$$+ \frac{0.04771190512}{\exp(1.005654552 \cdot \sigma_{0.2} - 0.4563315874 \cdot \sigma_u - 0.1039207902 \cdot T - 0.0006274577723 \cdot \dot{\varepsilon} - 59.20988646) + 1.0}$$
$$+ \frac{1.71252668}{\exp(0.4536180027 \cdot \sigma_u - 0.1283652688 \cdot \sigma_{0.2} - 0.4198358056 \cdot T - 0.01257380184 \cdot \dot{\varepsilon} - 56.939743) + 1.0}$$
$$- 0.195416497$$

For the parameter $m_{lead}\,(T, \dot{\varepsilon}, \sigma_{0.2}, \sigma_u)$ the MFNN function is:

$$m_{lead}\,(T, \dot{\varepsilon}, \sigma_{0.2}, \sigma_u) =$$
$$= \frac{3.643881706}{\exp(0.6385643297 \cdot T - 0.2022424958 \cdot \sigma_u - 0.6227643831 \cdot \sigma_{0.2} - 0.1053848883 \cdot \dot{\varepsilon} - 77.21535061) + 1.0}$$
$$- \frac{9.884337419}{\exp(0.01629318253 \cdot \sigma_{0.2} - 0.007234343592 \cdot \sigma_u + 0.0007329634094 \cdot T + 0.0001456651298 \cdot \dot{\varepsilon} - 1.455770771) + 1.0}$$
$$+ \frac{0.08146039906}{\exp(0.4112705698 \cdot \sigma_{0.2} - 0.3970669265 \cdot \sigma_u - 0.3081988387 \cdot T + 0.3491973275 \cdot \dot{\varepsilon} + 38.95247934) + 1.0}$$
$$+ \frac{7.106945027}{\exp(0.4026283571 \cdot \sigma_{0.2} + 0.4217960215 \cdot \sigma_u - 0.8012441872 \cdot T + 0.07559427212 \cdot \dot{\varepsilon} - 37.3985282) + 1.0}$$
$$+ \frac{1.621509654}{\exp(0.3513192334 \cdot \sigma_{0.2} + 0.09960028714 \cdot \sigma_u - 0.7307116249 \cdot T + 0.2176743567 \cdot \dot{\varepsilon} + 69.50970479) + 1.0}$$
$$+ 0.6084863663$$

The predictions of functions (12) and (13) are represented in Fig. 8, where a good agreement with the corresponding values from the test matrix can also be found.

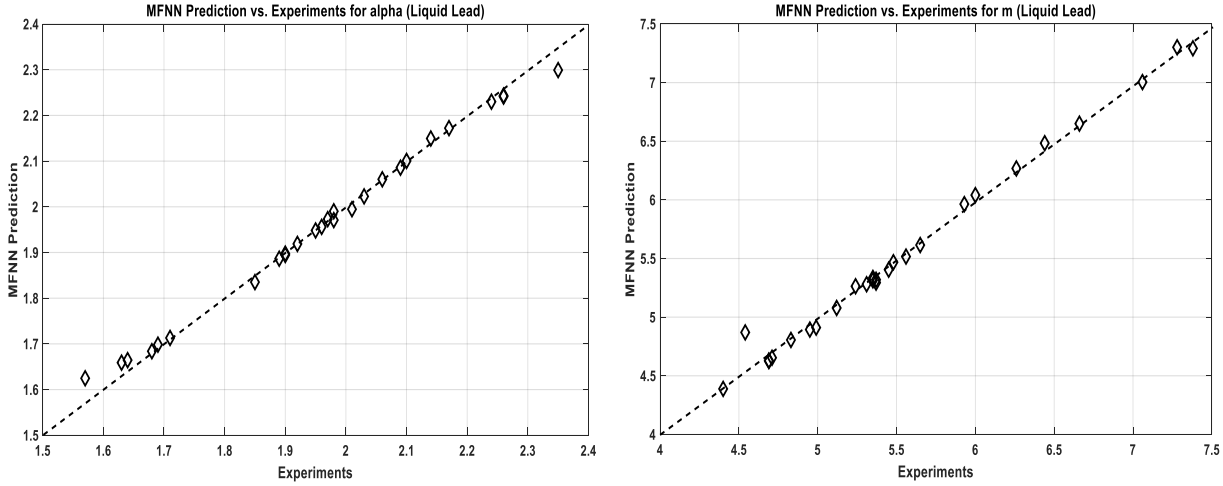

Figure 8. Predictions of the function $\alpha_{lead}\,(T, \dot{\varepsilon}, \sigma_{0.2}, \sigma_u)$ (a) and of the function $m_{lead}(T, \dot{\varepsilon}, \sigma_{0.2}, \sigma_u)$ (b) versus experimental values.

Some comments are needed regarding the prediction accuracy of the MFNN model for α and m values compared to the experiments performed in the liquid lead environment. It was found from the preliminary analysis a considerable scattering for the values of the parameters α and m, both for the air environment (Fig. 2) and, especially, for the liquid lead environment (Fig. 3). However, modelling by the method of artificial neural networks of the MFNN type leads to obtaining fairly accurate prediction functions for α and m, a remarkable fact all the more since they are based on four modelling parameters: temperature, deformation rate, yield stress, the maximum load corresponding to the localized deformation. Such modelling, in which several input parameters enter, is very difficult to achieve with the usual fitting methods that are provided in the statistical packages of various programs.

5. APPLICATION OF RAMBERG-OSGOOD MFNN MODEL TO ASSESS THE STRESS-STRAIN BEHAVIOUR OF 316L IN THE AIR AND IN THE LIQUID LEAD ENVIRONMENTS AT THE TEMPERATURE OF 375ºC

In the following, an application of the MFNN functions regarding the Ramberg-Osgood relationship will be presented, in which the prediction of the Ramberg-Osgood type

mechanical stress-strain curve of 316L samples in the liquid lead at 375°C is evaluated, compared to the mechanical behaviour in the air at the same temperature. From the test matrix, we will choose the SSRT-type tests in air and liquid lead. From the equations obtained for the parameters of the Ramberg-Osgood relationship, we will obtain the numerical values for the analyzed situation.

At the same time, to study the difference between the experimental curves in air and liquid lead media and those predicted by the solutions of the Ramberg – Osgood equation, the statistical parameters residuals and standardized residuals are used [14], which are described below.

The residual parameter is defined:

$$Residual = \sigma_{exp} - \sigma_{pred} \tag{14}$$

where:

σ_{exp} – Experimental value of mechanical stress;

σ_{pred} – The predicted (estimated) value of the mechanical stress.

The standardized residual parameter is the ratio of the individual raw residual to the standard deviation. The residual standard deviation is defined as:

$$\mathrm{S_{res}} = \sqrt{\frac{\sum\left(\sigma_{\mathrm{exp}} - \sigma_{\mathrm{pred}}\right)^2}{\mathrm{N} - 2}} \tag{15}$$

with:

$\mathrm{S_{res}}$ - Residual standard deviation;

N – Number of evaluation points.

The standardized residual provides a measure of the prediction error:

$$Standardized\ Rezidual = \frac{Residual}{S_{res}} \tag{16}$$

In the scientific literature [15] it is mentioned that the standardized residual must respect the inequality $\mathrm{S_{res}} < 3$, to have an adequate prediction.

For the prediction of the tests carried out in the air environment, we apply the following conditions to obtain the numerical values of the parameters of the Ramberg-Osgood relationship in the analyzed case study:

- Temperature 375 ($units\ ^{o}C$);
- Strain rate $\dot{\varepsilon} = 5\ (units\ 10^{-5}\ s^{-1})$;
- Yield stress $\sigma_{0.2} = 221\ (units\ MPa)$;
- Maximum stress at necking $\sigma_u = 497\ (units\ MPa)$.

Using Equation (10) we get:

$$\alpha_{air}\ (T, \dot{\varepsilon}, \sigma_{0.2}, \sigma_u) = \alpha_{air}\ (375, 5, 221, 497) = 1.75 \tag{17}$$

Analogous for the coefficient m (Equation 11) get:

$$m_{air}\ (T, \dot{\varepsilon}, \sigma_{0.2}, \sigma_r) = m_{air}\ (375, 5, 221, 497) = 5.55 \tag{18}$$

Thus, in air, the equation of the Ramberg-Osgood mechanical stress-strain curve for 316L at 375°C becomes:

$$\frac{\varepsilon}{\varepsilon_0} = \frac{\sigma}{\sigma_0} + 1.75 \cdot \left(\frac{\sigma}{\sigma_0}\right)^{5.55} \tag{19}$$

It is useful to mention that, if we use the approach from ASTM E646-07 [15] to obtain the deformation hardening coefficient, for tests in the air environment, the value is $m = 4.1$, which is of the same order of magnitude as the one obtained above. It should also be noted that in ASTM E646-07 an error of results between 5% and 15% is mentioned.

To verify the accuracy of the prediction, a comparison between the values of the experimental mechanical stress-strain curve and those given by Equation 19 for the air environment is shown in Fig. 9a. At the same time, Fig. 9b shows the residual and standardized residual parameters.

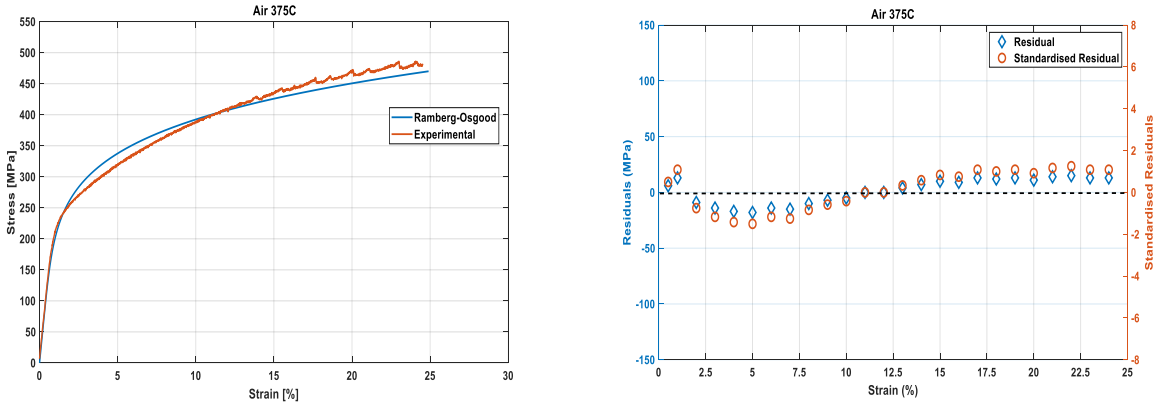

(a) (b)

Figure 9. Comparison between the experimental mechanical stress-strain curve and the Ramberg-Osgood relationship for SSRT tests in the air at 375°C (a) and the residual and standardized residual parameters (b) (S_res<3).

For the tests carried out in the liquid lead environment we apply the conditions:

- Temperature 375 ($units\ ^oC$);
- Strain rate $\dot{\varepsilon} = 5(units\ 10^{-5}\ s^{-1})$;
- Yield stress $\sigma_{0.2} = 209\ (units\ MPa)$;
- Maximum stress at necking $\sigma_r = 462\ (units\ MPa)$.

Using the equation for the parameter α obtained within the MFNN (Equation 12) we obtain:

$$\alpha_{Lead}\ (T, \dot{\varepsilon}, \sigma_{0.2}, \sigma_r) = \alpha_{Lead}\ (375, 5, 209, 462) = 1.83 \tag{20}$$

Analogous for m (Equation 13) we get:

$$m_{Lead}\ (T, \dot{\varepsilon}, \sigma_{0.2}, \sigma_r) = m_{Lead}\ (375, 5, 209, 462) = 5.61 \tag{21}$$

In the liquid lead environment, the Ramberg-Osgood mechanical stress-strain curve equation for 316L stainless steel at 375°C becomes:

$$\frac{\varepsilon}{\varepsilon_0} = \frac{\sigma}{\sigma_0} + 1.83 \cdot \left(\frac{\sigma}{\sigma_0}\right)^{5.61} \tag{22}$$

With the approach in ASTM E646-07, for the coefficient of deformation hardening, for tests in the liquid lead environment, the value is $m = 3.4$, of the same order of magnitude as that obtained above.

Fig. 10a shows a comparison between the values of the experimental mechanical stress-strain curve and those predicted by the equation Equation (22) for the liquid lead medium, and Fig. 10b shows the residual parameters and the associated standardized residuals.To perform crack initiation and propagation, the model takes into account the extinction of finite elements from the crack front. The fact is performed by de-cohesion when the achievement of the critical fraction of voids in the area is reached. The extinction of the finite elements on the front of the advancing crack happens when the material cohesion achieves the critical fraction of voids.

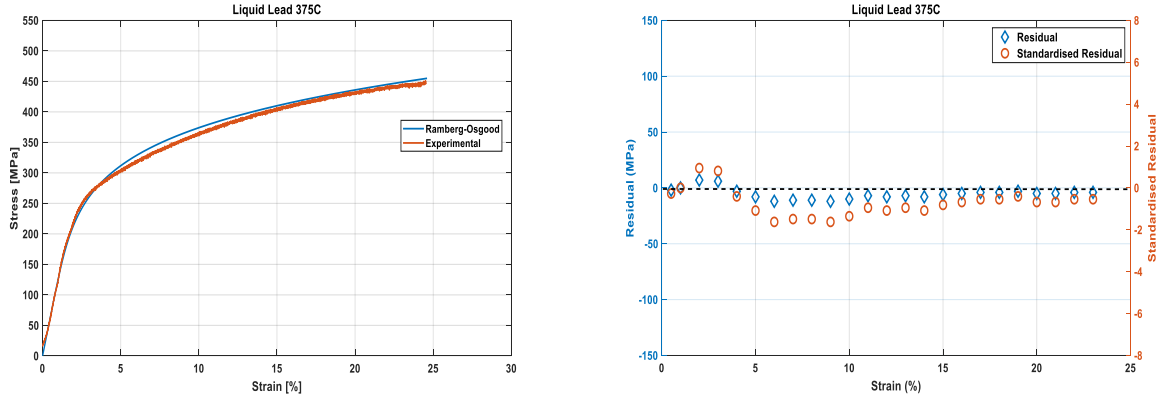

(a) **(b)**

Figure 10. Comparison between the experimental mechanical stress-strain curve and the Ramberg-Osgood relationship for SSRT tests in the liquid lead at 375°C (a) and the residual and standardized residual parameters (b) ($S_{res} < 3$).

It can be seen that the Ramberg - Osgood equation (22) provides the predictions in agreement with the experimental data obtained in the liquid lead environment, for the corresponding deformation range ($S_{res} < 3$).

In this context, the following benefits of the method developed in this work, for obtaining the Ramberg - Osgood parameters, can be highlighted:

- the method is easy to implement in programming environments (MATLAB), and the numerical solution of the transcendental equation for the deformation hardening coefficient is more flexible and faster than existing solutions in other methodologies;

- the parameters α and n obtained with the presented method can describe the domain of the experimental curves $\sigma = f(\varepsilon)$ expressed by the Ramberg – Osgood relation, up to the maximum load corresponding to the localized deformation, σ_u;

- the prediction accuracy was checked with statistical parameters residuals and standardized residuals, and the results were quite good.

It should be noted in this context that, in general, the behaviour of stainless steel in the liquid lead is somewhat different than in other metallic environments, as the embrittlement in this test environment is not as severe compared to most other materials [16]. Thus, Hamouche-Hadjem observed some differences in fracture morphology for 316L steel exposed in Pb-Bi [17].

6. CONCLUSIONS

Romania, through RATEN ICN, is involved in the construction of the ALFRED demonstrator (Advanced Lead Fast Reactor European Demonstrator), in which the core of the reactor uses cooling in the liquid lead environment. This constitutes one of the arguments for the development of studies on innovative materials of generation IV, having the stated objective of the problem of the contact between the liquid lead and the structural materials specific to this type of reactor.

The purpose of this paper is to highlight the changes in the thermomechanical behaviour induced by the contact between the 316L austenitic steel with liquid lead, as well as its modelling through the equations of the Ramberg-Osgood type mechanical stress-strain curves. The conclusions of the work can be summarized as follows:

- The tensile tests in air and liquid lead were carried out at deformation rates of the sample in the range $\dot{\varepsilon} = (10^{-3}, 10^{-5})s^{-1}$, in accordance with ASTM G129 și ASTM E8 , in a range of temperatures 350°C - 400°C.

- Using the methodology described in the paper, the following quantities were extracted from the $\sigma = f(\varepsilon)$ curves: the coefficient α of the Ramberg-Osgood relationship, the parameter m, which is the inverse of the hardening exponent, n. At the same time, the database also contains the values of the yield stress, $\sigma_{0.2}$, respectively of the maximum load corresponding to the localized deformation, σ_u, determined for all tested samples.

- In the paper, a model is developed based on the experimental results carried out in the liquid lead environment, compared to the air environment, which allows obtaining some analytical equations for the coefficients of the Ramberg-Osgood-type mechanical stress-strain curve equation. Thus, to highlight the changes induced by the contact with liquid lead on the thermomechanical behaviour of the 316L steel, the artificial neural network method, of the "Multilayer Feedforward Neural Network" type, was used in the processing of the experimental database. The obtained constitutive equation of the Ramberg-Osgood type is applied for the air environment and the liquid lead environment at a temperature of 375°C and includes the following parameters as input: temperature, deformation rate, yield stress, the maximum stress corresponding to the localized deformation.

- The two Ramberg-Osgood type equations obtained for the air environment and the liquid lead environment at the temperature of 375°C were verified to the experimental data and a very good prediction agreement was obtained. Thus, the developed model has practical utility in the structural integrity analysis of the various components made of 316L steel in the ALFRED reactor.

Future research directions and the remaining open research issues are mentioned in the next. For the embrittlement phenomenon of 316L steel in liquid lead, specific to the ALFRED reactor, an open issue will be establishing the influence of oxygen on this mechanism. After performing the experimental tests, similar to this study, but with the monitoring of the oxygen concentration in the liquid lead, the database will be updated, and the oxygen concentration will also enter the input parameter of the MFNN network. Therefore, the prediction functions for the parameters of the Ramberg-Osgood equation will be properly updated to use this equation to evaluate the structural integrity through the analysis with the finite element method of the ALFRED components prone to the LME mechanism.

Acknowledgements: *The authors express their full gratitude to the Nuclear Research Institute, Pitesti, Romania, which facilitated the conduct of the experiments in specialized laboratories.*

REFERENCES

[1] Xing-G, *Liquid Metal Embrittlement of a 9Cr-1Mo Ferritic-martensitic Steel in Lead-bismuth Eutectic Environment under Low Cycle Fatigue*, Belgium, November 2015.
[2] Ralph, P. Papirno, *Computer analysis of stress data: program description and user instructions*, Army Materials and Mechanics Research Center Watertown, Massachusetts, 1976.
[3] Rajendran, R., Venkateshwarlu, M., Petley, V., Verma, S., *Journal Mechanical Behaviour Materials*, **23** (3-4), 101, 2014.
[4] Pranav, S.P., Rajprasad, Nalavdea, A.R, Kujawski, D., *Procedia Structural Integrity*, **17**, 750, 2019.
[5] ASTM G129-00, *Standard Practice for Slow Strain Rate Testing to Evaluate the Susceptibility of Metallic Materials to Environmentally Assisted Cracking*, 2000.
[6] ASTM E8/E8M, *Test Methods for Tension Testing of Metallic Materials*, 2009.
[7] Dieter, G. Jr., *Mechanical Metallurgy*, McGraw-Hill Book Company, 1961.
[8] Stoica, L., Radu V., Nitu A., Prisecaru, I., *Journal of Science and Arts*, **3** (56), 831, 2021.
[9] Matlab R2017b, *The MathWorks*, Inc., USA, 2017.
[10] Taha, M.M.R., Noureldin, A., El-Sheim, N., Shrive, N.G., *Canadian Journal of Civil Engineering*, **30** (3), 523, 2011.
[11] Jung, S., Ghaboussi, J., *Computers and Structures*, **84** (15-16), 955, 2006.
[12] Wang, N., Tu, S.T., Xuan, F.Z., *Engineering Failure Analysis*, **31**, 302, 2013.
[13] Bhadeshia, H.K.D.H., *ISIJ International*, **39** (10), 966, 1999.
[14] Hessling, J.P. *Uncertainty Quantification and Model Calibration Paperback*, InTechOpen, London, UK, 2017.
[15] ASTM E646-07, *Standard Test Method for Tensile Strain-Hardening Exponents (n - Values) of Metallic Sheet Materials*, 2007.
[16] Kolman, D.G., *Journal of Science and Engineering*, **75**(1), 42, 2019.
[17] Hamouche-Hadjem, Z., Auger, T., Guillot, I., Gorse, D., *Journal of Nuclear Materials*, **376**(3), 317, 2008.